



FULL PAPER

In silico characterization of ligand–receptor interactions for U-47700, *N,N*-didesmethyl-U-47700, U-50488 at mu- and kappa-opioid receptors

Antonio Laus¹ | Amit Kumar²  | Pierluigi Caboni³ | Maria A. De Luca¹ | Michael H. Baumann⁴ | Enrico Pieroni⁵ | Graziella Tocco³ 

¹Department of Biomedical Sciences, University of Cagliari, Cittadella Universitaria di Monserrato, Cagliari, Italy

²Department of Electrical and Electronic Engineering, University of Cagliari, Cagliari, Italy

³Department of Life and Environmental Sciences, University of Cagliari, Cittadella Universitaria di Monserrato, Cagliari, Italy

⁴Designer Drug Research Unit, Intramural Research Program, National Institute on Drug Abuse, National Institutes of Health, Baltimore, Maryland, USA

⁵CRS4, Modelling, Simulation and Data Analysis Program, Pula, Italy

Correspondence

Graziella Tocco, Department of Life and Environmental Sciences, University of Cagliari, Cittadella Universitaria di Monserrato, Monserrato, 09042 Cagliari, Italy.

Email: tocco@unica.it

Amit Kumar, Department of Electrical and Electronic Engineering, University of Cagliari, 09123 Cagliari, Italy.

Email: amit.kumar@unica.it

Present address

Antonio Laus, Department of Life Sciences, University of Modena and Reggio Emilia, Modena, Italy.

Funding information

NIDA grant DA-000523-14; JUST-2017-AGDRUG SUPPORTING INITIATIVES IN THE FIELD OF DRUGS POLICY Grant agreement n. 806996-JUSTSO; Sardegna Ricerche and Sardinia Region

Abstract

The increasing misuse of novel synthetic opioids (NSOs) represents a serious public health concern. In this regard, U-47700 (*trans*-3,4-dichloro-*N*-[2-(dimethylamino)cyclohexyl]-*N*-methylbenzamide) and related “U-compounds” emerged on recreational drug markets as synthetic substitutes for illicit heroin and constituents of counterfeit pain medications. While the pharmacology of U-compounds has been investigated using in vitro and in vivo methods, there is still a lack of understanding about the details of ligand–receptor interactions at the molecular level. To this end, we have developed a molecular modeling protocol based on docking and molecular dynamics simulations to assess the nature of ligand–receptor interactions for U-47700, *N,N*-didesmethyl U-47700, and U-50488 at the mu-opioid receptor (MOR) and kappa-opioid receptor (KOR). The evaluation of ligand–receptor and ligand–receptor-membrane interaction energies enabled the identification of subtle conformational shifts in the receptors induced by ligand binding. Interestingly, the removal of two key methyl groups from U-47700, to form *N,N*-didesmethyl U-47700, caused a loss of hydrogen bond contact with tryptophan (Trp)229, which may underlie the lower interaction energy and reduced MOR affinity for the compound. Taken together, our results are consistent with the reported biological findings for U-compounds and provide a molecular basis for the MOR selectivity of U-47700 and KOR selectivity of U-50488.

Abbreviations: Asn, asparagine; Asp, aspartate; Gln, glutamine; His, histidine; Ile, isoleucine; KOR, kappa-opioid receptor; Lys, lysine; MD, molecular dynamics; Met, methionine; MOR, mu-opioid receptor; NAMD, nanoscale molecular dynamics; NPT, number of atoms, pressure, and temperature run; OPLS, optimized potentials for liquid simulations; POPC, palmitoyl-oleoyl-phosphatidyl-choline; RMDE, receptor membrane discrimination energy; RSDE, receptor specificity discrimination energy; TM, transmembrane; Trp, tryptophane; Tyr, tyrosine; U-47700, (*trans*-3,4-dichloro-*N*-[2-(dimethylamino)cyclohexyl]-*N*-methylbenzamide); U-50488, *trans* 2-(3,4-dichlorophenyl)-*N*-methyl-*N*-[2-(pyrrolidinyl)cyclohexyl]acetamide; Val, valine.

This is an open access article under the terms of the Creative Commons Attribution-NonCommercial-NoDerivs License, which permits use and distribution in any medium, provided the original work is properly cited, the use is non-commercial and no modifications or adaptations are made.

© 2023 The Authors. *Archiv der Pharmazie* published by Wiley-VCH GmbH on behalf of Deutsche Pharmazeutische Gesellschaft.

KEYWORDS

docking and molecular dynamics, ligand-receptor-membrane interaction analysis, mu and kappa- opioid receptors, U-compounds

1 | INTRODUCTION

Ever since the discovery of opioid receptors and endogenous opioid peptides,^[1] biomedical scientists have searched for morphine-like analgesic agents with reduced adverse effects. From the mid-1970s onward, medicinal chemists synthesized thousands of novel synthetic opioids belonging to different chemical classes.^[2–5] In this regard, *trans*-3,4-dichloro-*N*-[2-(dimethylamino)cyclohexyl]-*N*-methylbenzamide (U-47700), *trans*-2-(3,4-dichlorophenyl)-*N*-methyl-*N*-[2-(pyrrolidinyl)cyclohexyl]acetamide (U-50488), and related “U-compounds” were developed by the Upjohn Company as potential pain medications. None of the U-compounds was ever approved for clinical use, but U-47700 and U-50488 are among the most selective compounds available for the mu-opioid receptor (MOR) and kappa-opioid receptor (KOR).^[6–8] From a chemical perspective, U-compounds display a strategic 1,2-ethylene diamine core that is also present in molecules with a wide variety of receptor activities.^[9] More precisely, the U-compounds all possess a *N*-(2-ethylamino) amide unit, with a sp^3 hybridized strongly basic nitrogen and a sp^2 hybridized polar nitrogen connected to two hydrophobic sites such as the cyclohexyl and phenyl moieties (Figure 1).

It was first observed by Szmuszkovicz^[11] that the introduction of an extra methylene (i.e., CH_2) group between the aromatic ring and

carbonyl moiety in the U-compounds scaffold (e.g., as in U-50488) produces a marked switch in selectivity from MOR to KOR, and this phenomenon has been called the “eastern methylene group effect.” The additional methylene group enables the portion of the molecule between the basic nitrogen atom and the amide group to adopt the torsional angle of 60° in a low-energy conformation necessary for a selective interaction with KOR.^[12] Conversely, the absence of the extra methylene (e.g., as in U-47700) holds the basic nitrogen and the aromatic ring in a spatial orientation similar to that of morphine.^[13] As a result, U-47700 is 10 times more potent in vivo than morphine as an analgesic agent, with high affinity and selectivity for MOR.^[10,11,14]

Beginning in 2015, U-47700 started appearing in recreational drug markets as a substitute for illicit heroin and a constituent of counterfeit pain medications.^[15,16] Since that time, U-47700 has been associated with hundreds of overdose fatalities, and the drug is now banned by national and international drug control laws.^[17,18] Human forensic studies show that U-47700 is biotransformed in vivo by stepwise removal of methyl groups from the basic nitrogen to yield *N*-desmethyl and *N,N*-didesmethyl metabolites.^[19] Notably, the removal of both methyl groups in *N,N*-didesmethyl U-47700 results in an almost complete loss of receptor binding affinity at MOR,^[10,14] along with a pronounced reduction in efficacy (Figure 1).^[20] Although the pharmacokinetic and pharmacodynamic properties of

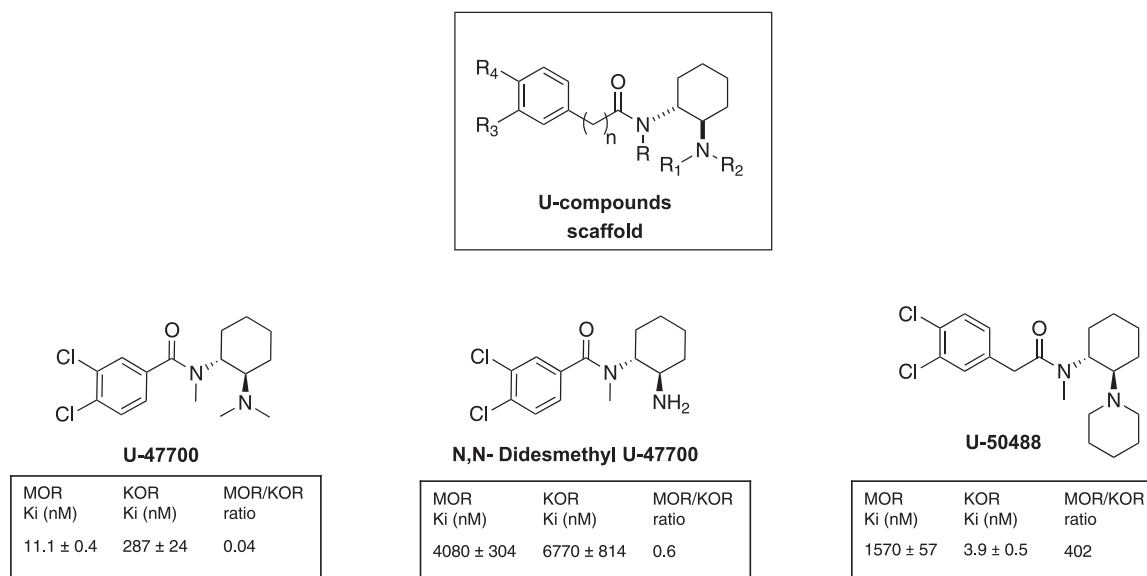


FIGURE 1 The U-compound scaffold: chemical structures for U-47700, *N,N*-didesmethyl U-47700, and U-50488 along with their respective binding affinities at MOR and KOR (data from Truver et al.^[10]). KOR, kappa-opioid receptor; MOR, mu-opioid receptor; U-47700, *trans*-3,4-dichloro-*N*-[2-(dimethylamino)cyclohexyl]-*N*-methylbenzamide; U-50488, *trans* 2-(3,4-dichlorophenyl)-*N*-methyl-*N*-[2-(pyrrolidinyl)cyclohexyl]acetamide.

U-compounds have been explored, very few reports have used *in silico* methods to characterize ligand–receptor interactions.^[13] Thus, in the present study, we examined ligand–receptor interactions for U-compounds at MOR and KOR using receptor models^[21,22] based on available crystallographic structures of *Mus musculus* MOR (PDB ID 6DDF)^[23] and *Homo sapiens* KOR (PDB ID 6VI4),^[24] both coupled to their G-proteins. The models were further utilized to analyze the dynamics of receptor–ligand interactions. Energetically favorable poses derived from the docking studies were employed in molecular dynamic (MD) simulations that allowed us to identify affinities, dominant interactions, and conformational changes associated with the ligand–receptor complexes.

2 | RESULTS AND DISCUSSION

2.1 | Molecular docking

Binding mode investigations were explored via custom-built MOR and KOR virtual models, using the Glide-XP docking protocol^[25,26] with U-47700, *N,N*-didesmethyl U-47700, and U-50488 as the target ligands. Using the most energetically favored docking poses allowed us to identify four specific regions of interaction for both MOR and KOR, and each ligand was investigated and classified on this basis. The MOR model is schematically shown in Figure 2.

The model was further validated by analyzing the poses for a set of 11 well-characterized fentanyl-derived compounds (see Supporting Information).

Specifically, we found an electrostatic region located on the transmembrane (TM)3 helix (A, Figure 2, red), two hydrophobic areas located along the inner (B, Figure 2, blue) and outer (C, Figure 2, green) regions of the orthosteric binding pocket, and a sterically hindered subpocket (D, Figure 2, yellow) located towards the opening of the main binding pocket, between the helices TM3 and TM5.

2.1.1 | MOR/U-compounds docking

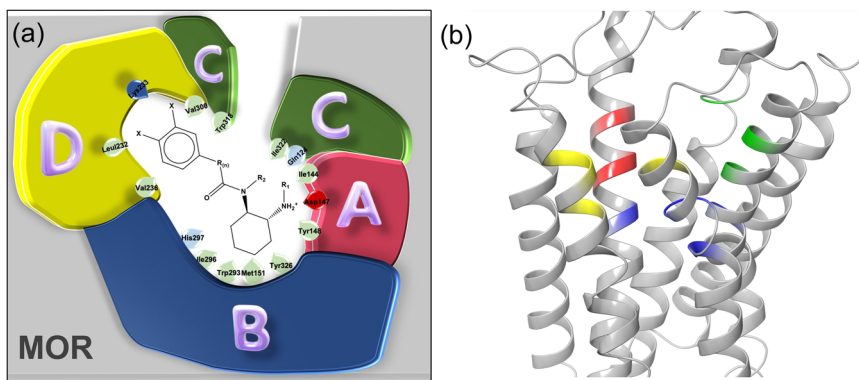
Analysis of docking poses revealed that the most important interactions occurred in MOR region A. In detail, we observed a salt

bridge between the positively charged amino group of the ligand and the negatively charged aspartate (Asp)147 on the receptor. This electrostatic interaction was observed for all the U-compounds under study, but key differences existed in the binding orientation of the ligands. Indeed, U-47700 was oriented towards the interior of the binding pocket (Figure 3a), whereas *N,N*-didesmethyl U-47700 (Figure 3b) and U-50488 (Figure 3c) preferentially targeted the outer region. In particular, the different orientation of *N,N*-didesmethyl U-47700 was related to a stronger ionic interaction at Asp147 due to the less hindered basic nitrogen. The longer and more flexible molecular chain was involved in the orientation of U-50488, which acquired additional Van der Waals interactions with the external region of the binding pocket. Additionally, a π -cation contact with tyrosine (Tyr)148 was observed for all ligands, with U-47700 displaying the strongest interaction and with U-50488 also involved in a π - π stacking with the same residue.

Region B represents the deepest part of the binding pocket where Van der Waals interactions mainly occur, especially with tyrosine (Tyr)326, tryptophan (Trp)293, and methionine (Met)151. This was particularly noticeable for U-47700 (Figure 3a) whose cyclohexyl and benzene ring moieties were involved in strong Van der Waals bonds. The same ligand also exhibited an important electrostatic free energy gain due to the significant interactions with the lateral side of the region located on TM6 and particularly with histidine (His)297. Strong Van der Waals interactions between the phenyl ring and isoleucine (Ile)296 were also observed. Conversely, *N,N*-didesmethyl U-47700 (Figure 3b) did not display such contacts with His297 and Ile296 but its amide methyl group was involved in Van der Waals interactions mainly with Met151 and scarcely with Trp293. In fact, the H-bond contact between the charged nitrogen of the ligand and the phenolic hydroxyl group of Tyr326, enabled the distancing of *N,N*-didesmethyl U-47700 from Trp293. Within region B, U-50488 (Figure 3c) displayed modest interactions with Met151 and Trp293 mediated by the amide methyl group. Conversely, significant Van der Waals connections were observed with His297 and Ile296, although the proximity of the amide oxygen of U-50488 and the imidazole ring of His297 was responsible of a steric effect.

Region C is the outer part of the MOR-binding region where isoleucine (Ile)322, glutamine (Gln)124, and tryptophan (Trp)318

FIGURE 2 (a) MOR docking regions for U-compounds: electrostatic (A), inner hydrophobic (B), outer hydrophobic (C), steric hindered subpocket (D). (b) Ribbon representation of ligand–MOR areas of interactions: region A (red), region B (blue), region C (green), and region D (yellow). MOR, mu-opioid receptor.



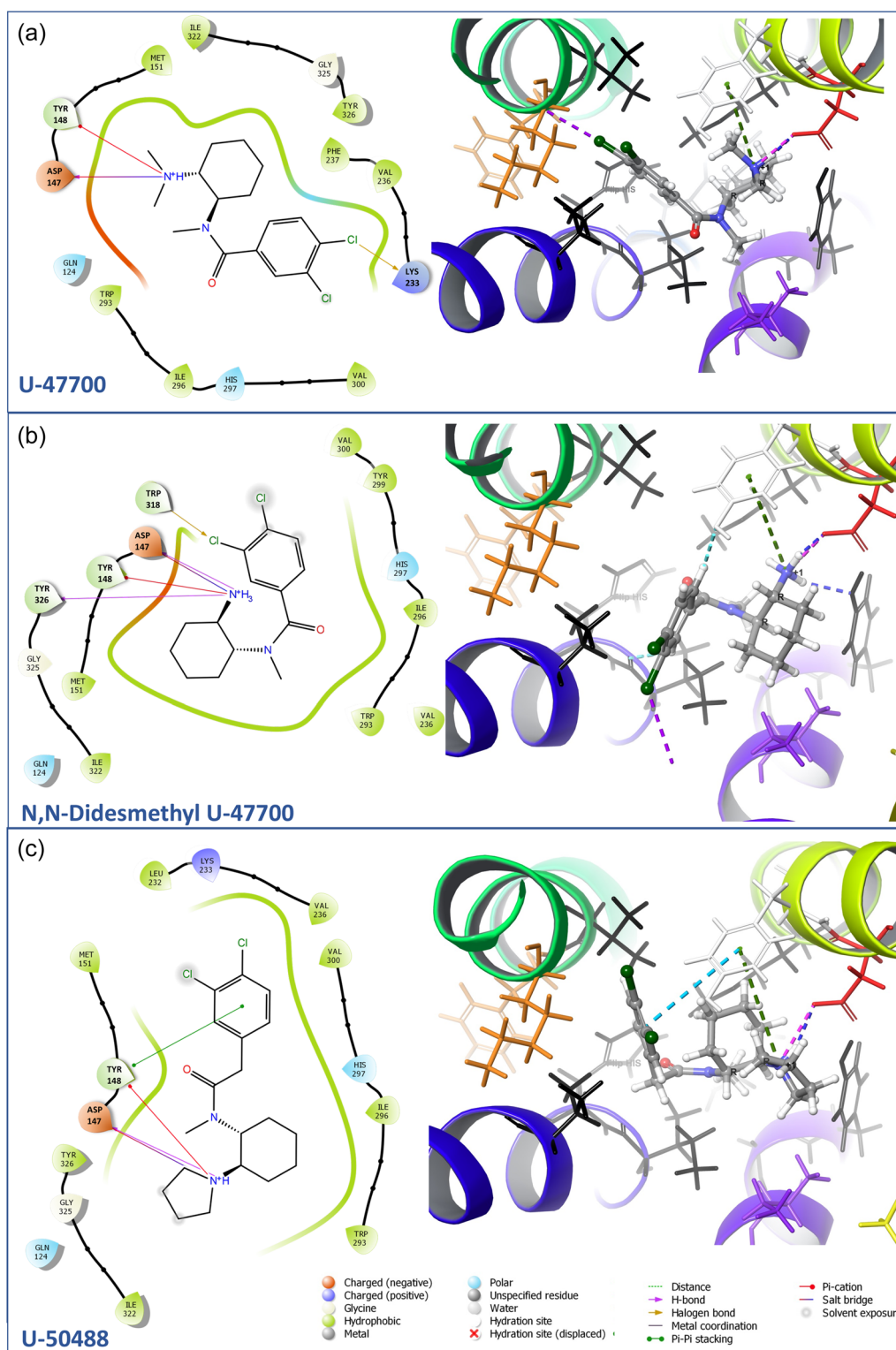
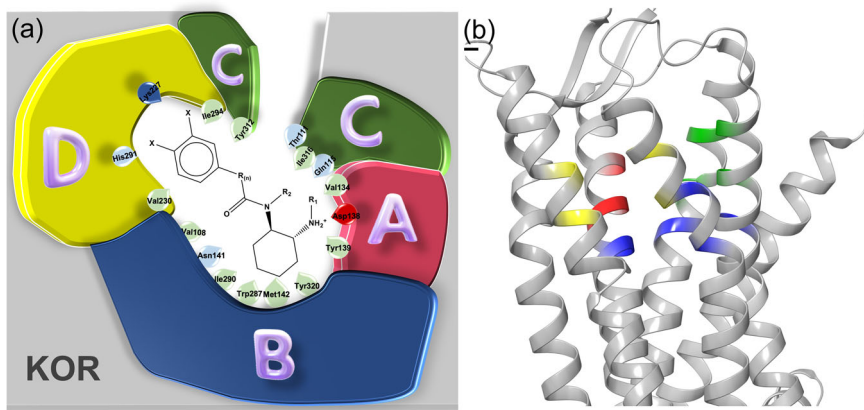


FIGURE 3 Glide-XP binding site molecular model of: (a) MOR/U-47700 complex; (b) MOR/*N,N*-didesmethyl U-47700 complex; (c) MOR/U-50488 complex. MOR, mu-opioid receptor; U-47700, *trans*-3,4-dichloro-*N*-[2-(dimethylamino)cyclohexyl]-*N*-methylbenzamide; U-50488, *trans* 2-(3,4-dichlorophenyl)-*N*-methyl-*N*-[2-(pyrrolidinyl)cyclohexyl]acetamide.

residues were involved in Van der Waals contacts, with very few electrostatic interactions. In detail, U-47700 (Figure 3a) engaged Van der Waals interactions via the methyl substituent of the amide group, particularly with Ile322 while *N,N*-didesmethyl U-47700 (Figure 3b)

and U-50488 (Figure 3c) gained contact with MOR through their cyclohexyl and aromatic moieties. Additionally, *N,N*-didesmethyl U-47700 was also involved in a halogen bonding with Trp318 (Figure 3b).

FIGURE 4 (a) KOR docking regions for U-compounds: electrostatic (A), inner hydrophobic (B), outer hydrophobic (C), steric hindered subreceptorial (D). (b) Schematic 3D representation of KOR docking regions for U-compounds. (B) Ribbon representation of ligand–KOR areas of interactions: region A (red), region B (blue), region C (green), and region D (yellow). 3D, three-dimensional; KOR, kappa-opioid receptor.



Finally, close to the outer part of the binding pocket, between helix TM5 and TM6, a sterically hindered subpocket region has been recognized and classified as region D. Residues lysine (Lys)233, leucine (Leu)232, valine (Val)236, and valine (Val)300 were specifically involved in electrostatic and Van der Waals interactions with the aromatic ring of U-47700. Interestingly, an additional halogen bond with Lys233 appeared significant in stabilizing U-47700 within this subpocket (Figure 3a). Quite distinctly, *N,N*-didesmethyl U-47700 did not enter in this receptor area, probably because of the strong interaction with region C (Figure 3b). Similarly, U-50488, due to its long chain and high flexibility, did not fit well into this subpocket (Figure 3c).

2.1.2 | KOR/U-compounds docking

An identical approach was adopted to investigate interactions for U-compounds and KOR (Figure 4). As already observed with MOR, the KOR model identified four different regions of interactions: the electrostatic region A (red) the inner and the outer regions B (blue) and C (green), and the subpocket region D (yellow).

A detailed depiction of KOR–ligand complexes is illustrated in Figure 5.

Again, the most important interaction between the positively charged amino group of the ligands and the negatively charged aspartate (Asp)138 of the receptor occurred in the electrostatic region A. As previously seen for MOR, this electrostatic interaction was observed for all the studied ligands, with very little difference regarding the orientation of the substituents of the basic nitrogen. Additionally, tyrosine (Tyr)139 and valine (Val)134 were also involved in Van der Waals bonding with the pyrrolidine residue of U-50488 (Figure 5a), the methyl groups on the basic nitrogen of U-47700 (Figure 5b), and the aromatic moiety of *N,N*-didesmethyl U-47700 (Figure 5c).

Within region B, Van der Waals interactions between the cyclohexyl moiety of U-50488 and residues tyrosine (Tyr)320, tryptophan (Trp)287, isoleucine (Ile)290 proved important. By analogy, asparagine (Asn)141 and methionine (Met)142 located on TM3 profitably interacted with the

pyrrolidine and the phenyl rings of U-504488 (Figure 5a). U-47700 also showed good contacts mediated by the alkyl substituents on the charged nitrogen and the aromatic portion (Figure 5b), while *N,N*-didesmethyl U-47700 (Figure 5c) was involved in H-bond with Asn141. Interestingly, the substituents on the amide nitrogen of U-50488 (Figure 5a) displayed strong Van der Waals interactions with residues isoleucine (Ile)316, glutamine (Gln)115, tyrosine (Tyr)325, and threonine (Thr)111 located in the outer region C.

Finally, with respect to U-47700 and *N,N*-didesmethyl U-47700, U-50488 showed the best pose within the subpocket of region D, because of a stable halogen bond with Lys 227. We also observed Van der Waals interactions between the aromatic region of U-50488 and histidine (His)291, valine (Val)230, and isoleucine (Ile)294 receptor residues (Figure 5a).

Overall, from the analysis of MOR docking poses, we can hypothesize that the different orientation of *N,N*-didesmethyl U-47700 and U-50488 with respect to U-47700, positioned further into the binding pocket and sub-pocket regions, might be responsible for their loss of MOR-binding affinity. In this regard, the strong ionic interaction of the unsubstituted basic nitrogen on *N,N*-didesmethyl U-47700 with the electrostatic region of the receptor, as well as the outward shift of U-50488 due its hindered amide substitution, seemed determinant. As already observed for MOR, a different ligand orientation within KOR was a key criterion for receptor affinity. It was observed that the additional methylene group of U-50488 moved the benzene ring to provide additional important contact with the outer region of the KOR binding pocket.

2.2 | Molecular dynamics

To shed light on the time-dependent chemical processes that cannot be addressed using laboratory-scale or static docking methods, we performed a series of molecular dynamics (MD) simulations to analyze the dynamics of both ligand–receptor and ligand–receptor–membrane complexes and to evaluate their interaction energies. Given the sizes of the systems studied (Table 1) and the required simulation computational

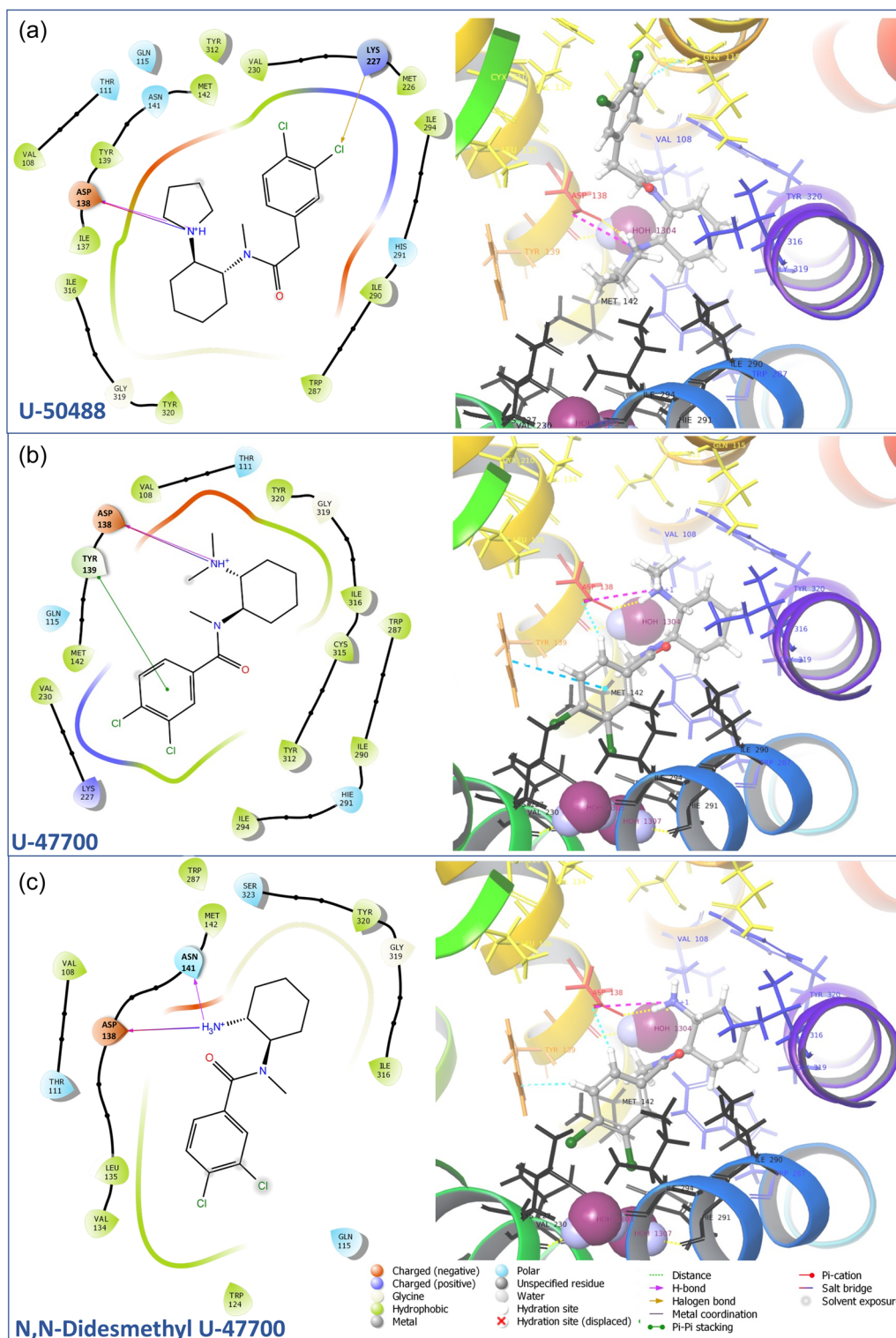


FIGURE 5 Glide-XP binding site molecular model of: (a) KOR/U-50488 complex; (b) KOR/U-47700 complex; (c) KOR/N,N-didemethyl U-47700 complex. KOR, kappa-opioid receptor; U-47700, *trans*-3,4-dichloro-*N*-[2-(dimethylamino)cyclohexyl]-*N*-methylbenzamide; U-50488, *trans* 2-(3,4-dichlorophenyl)-*N*-methyl-*N*-[2-(pyrrolidinyl)cyclohexyl]acetamide.

times, we focused our investigation on the affinities of U-47700 and U-50488 for MOR and KOR, to understand the selectivity difference (Table 1). The MOR-*N,N*-didesmethyl U-47700 complex (i.e., “NNd-U-47700” in Table 1) was also analyzed to evaluate the affinity change. As a

reference system, we also simulated the membrane-embedded and unbound MOR and KOR (referred to as “-Free” in Table 1).

Interaction energy calculations, although providing only a rough valuation of enthalpic contribution, proved to be affordable

TABLE 1 Summary of the simulations performed for the MOR and KOR free and bound to U-compounds.

System	Total number of atoms	Simulation box size (Å ³)	Simulation time (ns)
MOR/U-47700	107,949	138 × 92 × 86	100
MOR/U-50488	107,956	138 × 92 × 86	100
MOR-Free	107,907	138 × 92 × 86	100
KOR/U-47700	108,064	138 × 92 × 84	100
KOR/U-50488	108,252	138 × 92 × 84	100
KOR-Free	108,203	138 × 92 × 84	100
MOR/NNd-U-47700	107,943	138 × 92 × 84	140

Note: All receptors are embedded in a lipidic membrane. The system MOR/NNd-U-47700 was simulated for a longer time to elucidate a particular effect discussed later in this section.

Abbreviations: KOR, kappa-opioid receptor; MOR, mu-opioid receptor; U-47700, *trans*-3,4-dichloro-*N*-[2-(dimethylamino)cyclohexyl]-*N*-methylbenzamide; U-50488, *trans* 2-(3,4-dichlorophenyl)-*N*-methyl-*N*-[2-(pyrrolidinyl)cyclohexyl]acetamide.

TABLE 2 Interaction energies between receptor and membrane (second column) and between receptor and ligand (third column), for U-47700, U-50488, and *N,N*-didesmethyl U-47700 for both MOR and KOR.

Complex	Receptor–membrane (kcal/mol)	Receptor–ligand (kcal/mol)	Receptor–membrane discrimination energy (RMDE) (kcal/mol)	Receptor specificity discrimination energy (RSDE) (kcal/mol)
MOR/U-47700	-1765 ± 39	-126 ± 6		
MOR/U-50488	-1836 ± 40	-109 ± 7	+71	-17
MOR/ <i>N,N</i> -didesmethyl U-47700	-1925 ± 47	-110 ± 6		
MOR-Free	-1832 ± 39	-		
KOR/U-47700	-1932 ± 45	-106 ± 6		
KOR/U-50488	-1836 ± 42	-135 ± 6	+96	-29
KOR-Free	-1920 ± 49	-		

Note: It is also reported the receptor specificity discrimination energy (fourth column), that is the difference between receptor energy interaction with top ligand and with lower-scoring ligand (values in the third column). Notice the minus sign due to this convention on the subtraction order. The fifth column reports the receptor membrane discrimination energy, obtained similarly to the previous one from values in the second column. This time, notice the plus sign.

Abbreviations: KOR, kappa-opioid receptor; MOR, mu-opioid receptor; U-47700, *trans*-3,4-dichloro-*N*-[2-(dimethylamino)cyclohexyl]-*N*-methylbenzamide; RMDE, receptor–membrane discrimination energy; RSDE, receptor specificity discrimination energy; U-50488, *trans* 2-(3,4-dichlorophenyl)-*N*-methyl-*N*-[2-(pyrrolidinyl)cyclohexyl]acetamide.

estimators of the overall binding affinity. Therefore, they are considered a valuable tool for ranking various complexes according to their interaction energies.^[27–29]

Moreover, the interaction energies between U-47700 and U-50488 and MOR and KOR were calculated (Table 2, third column).

To indirectly highlight the subtle conformational changes induced by ligand docking, we also evaluated the interaction energy between the receptor and the membrane for complexed and uncomplexed (free) receptors (Table 2, second column). The rationale for this approach is that receptor contacts with the membrane are involved during interaction, and it has been shown that the membrane itself can be remodeled, in particular by altering its curvature and other biophysical properties.^[30–32] As a matter of fact, this approach is often used to elucidate the membrane–protein

interaction features.^[33] Thus, opioid receptors bound to U-compounds might influence protein interactions with the surrounding membrane. Small effects can be expected, based on the relative sizes of membrane lipids, receptor proteins, and ligands, yet membrane–complex interactions are often more sensitive than direct observation of changes in protein conformations (e.g., by root-mean-square deviation (RMSD) analysis) via MD trajectories.^[34] Moreover, as a distinct advantage, membrane–complex interaction analysis requires much shorter MD simulations. The receptor–membrane interaction energies for the MOR and KOR complexes are shown in the second column of Table 2.

To better understand the ligand–receptor interactions, we also studied their H-bond networks. Although both U-47700 and U-50488 bound to MOR displayed H-bond interactions with

Asp147 (region A) for more than 95% of MD simulations, a peculiar distinction was noted. More specifically, the backbone atoms of Asp147 were involved for 80% of the MD simulation time with U-47700, while backbone atom interactions were not involved with U-50488. For U-50488, the interactions of with Asp147 were dominated by interactions only with the sidechain atoms. This result is in full agreement with the docking analysis. In contrast to the H-bond interactions at MOR, a marked difference in the persistence of H-bond interactions was observed for U-47700 and U-50488 bound to KOR. We found a H-bond contact between sidechain atoms of residue Asn141 (region B) and U-47700 for 50% of the simulation time, while the same interaction persisted for up to 90% of the MD simulation between the sidechain atoms of residue Asp138 (region A) and U-50488.

The ligand–receptor interaction energies obtained by MD simulations (Table 2 third column) confirmed U-47700 and U-50488 as the top-ranking ligands for MOR and KOR, respectively. We refer to the difference in interaction energy between the same receptors complexed with top and lower-scoring ligands as the receptor specificity discrimination energy (RSDE). For MOR, the RSDE was -17 kcal/mol and for KOR it was -29 kcal/mol (Table 2, fourth column). Usually, MD is more reliable for affordable ranking than for accurately predicting binding energies, but as both these values were reasonably above the RMSD fluctuations and the thermal energy at simulation temperature, these values can be considered meaningful in that regard. Thus, RSDE seems to be able to discriminate between good and bad ligands for both MOR and KOR.

Furthermore, the interaction energy of the MOR with the membrane (Table 2, second column) was similar when the receptor was bound to U-50488 and when it was free: -1836 versus -1832 kcal/mol respectively, that is, 4 kcal/mol difference, which is roughly equivalent to RMSD and, therefore, less physically important. Conversely, as previously observed, a much better energy gain was observed for MOR bound to U-47700. That is, the worst MOR ligand engages the receptor very weakly, in a way comparable to the free receptor, confirming the ability of MD to discriminate ligand MOR receptor affinity.

We observed a similar situation for the ligand–KOR–membrane system, where the receptor–membrane interaction energies were similar for KOR bound to U-47700 versus free (12 kcal/mol difference), while KOR bound to U-50488 displayed a stronger contact. In this case, this difference is above system thermal fluctuations but less than KOR receptor–membrane discrimination energy (RMDE), as previously discussed.

We refer to the difference in receptor–membrane interaction energy between the same receptor complexed to the highest and lowest-scoring ligand complexes as RMDE. For the KOR system RMDE was 96 kcal/mol and for the MOR system it was 71 kcal/mol (Table 2, fifth column). Therefore, RMDE values are quite large, approximately 3–4 times the respective RSDE, and thus, being above the RMSD fluctuations and the thermal energy at simulation temperature, can be considered physically meaningful. As a matter

of fact, also RMDE seems to be able to discriminate about good and worst ligand for both MOR and KOR.

By comparison, for the low-scoring ligand, as previously observed, the bound and free states were very close in energy, with a gap of only 12 kcal/mol for KOR and 4 kcal/mol for MOR, below their respective RMDE.

To better understand why even minor changes in ligand structure could dramatically influence receptor affinities, we also simulated the *N,N*-didesmethyl U-47700 bound to MOR. The interaction energy between the ligand and MOR was -110 kcal/mol (Table 2), similar to the energy for U-50488 at MOR (-109 kcal/mol), and much less favorable when compared to -126 kcal/mol observed for U-47700 (Table 2). The time evolution of the interaction energy for *N,N*-didesmethyl U-47700 (Figure 6a) showed a rather peculiar profile.

In particular, around the simulation time of $t = 50$ ns, the interaction energy rapidly changed from ≈ -130 to ≈ -110 kcal/mol in about 20 ns, when the *N,N*-didesmethyl derivative switched its configuration and achieved a final interaction energy similar to that of U-50488. To confirm the persistence of this effect and to gain more insight into it, we prolonged the total simulation time up to 140 ns. Furthermore, plotting the dihedral angles of the ligand backbone during simulation experiments (Figure 7), we were able to identify a distinct transition with a sudden 90° angle change around the simulation time $t = 45$ ns. The interaction energy between MOR and the membrane (Figure 6b) was also analyzed during simulation, showing an energy jump from ≈ -1600 to ≈ -2000 kcal/mol around the simulation time $t = 30$ ns, thereby anticipating the ligand conformational switch. To gain more insight into the observed effect for this system, we extended the total simulation time up to 140 ns. In this way we confirmed the persistence of the conformational change, that is, the system did not switch back and forth between the two conformations. Moreover, we accumulated more statistics to reduce estimated free energy errors.

This effect confirmed the sensitivity and rapidity of the ligand–receptor–membrane interaction analysis as a tool to highlight subtle, but functionally relevant, changes in ligand orientation or binding pose. Notably, the ligand configuration transition from compact to extended conformation was extremely quick. Nevertheless, such a switch was not evident immediately after the dynamics started but required a longer simulation period to be sampled.

Importantly, none of the best poses from the docking analysis detected for this ligand predicted this extended binding configuration.

To investigate the potential role of the energy transition observed for *N,N*-didesmethyl U-47700 on its reduced affinity at MOR, we also evaluated the H-bond network between receptor and ligand for the two major conformations detected at different ranges of MD simulation time (Table 3).

The H-bonds were considered persistent if they were present for more than 20% of the simulation period. Specifically, the reduction in interaction energy between the ligand and the receptor can be attributed to the loss of H-bond interaction between residue Trp229 and *N,N*-didesmethyl U-47700 and to the

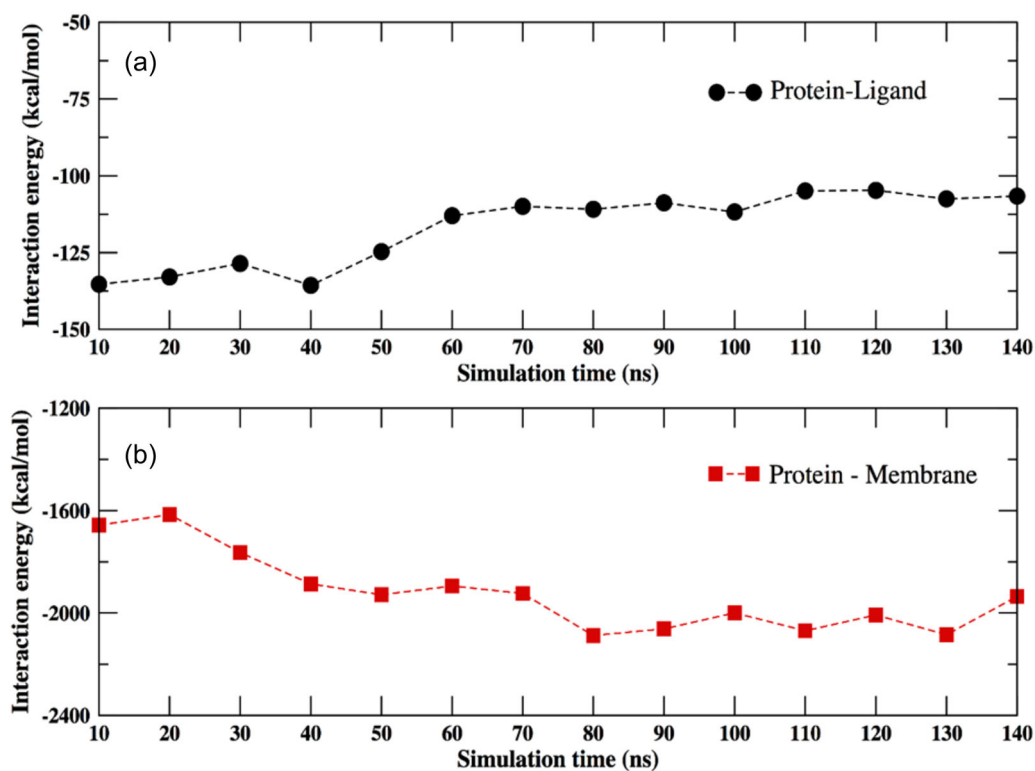


FIGURE 6 Time evolution of the interaction energy (a) between the ligand *N,N*-didesmethyl U-47700 and MOR, and (b) between MOR (docked to *N,N*-didesmethyl U-47700) and membrane. MOR, mu-opioid receptor; U-47700, *trans*-3,4-dichloro-*N*-[2-(dimethylamino) cyclohexyl]-*N*-methylbenzamide.

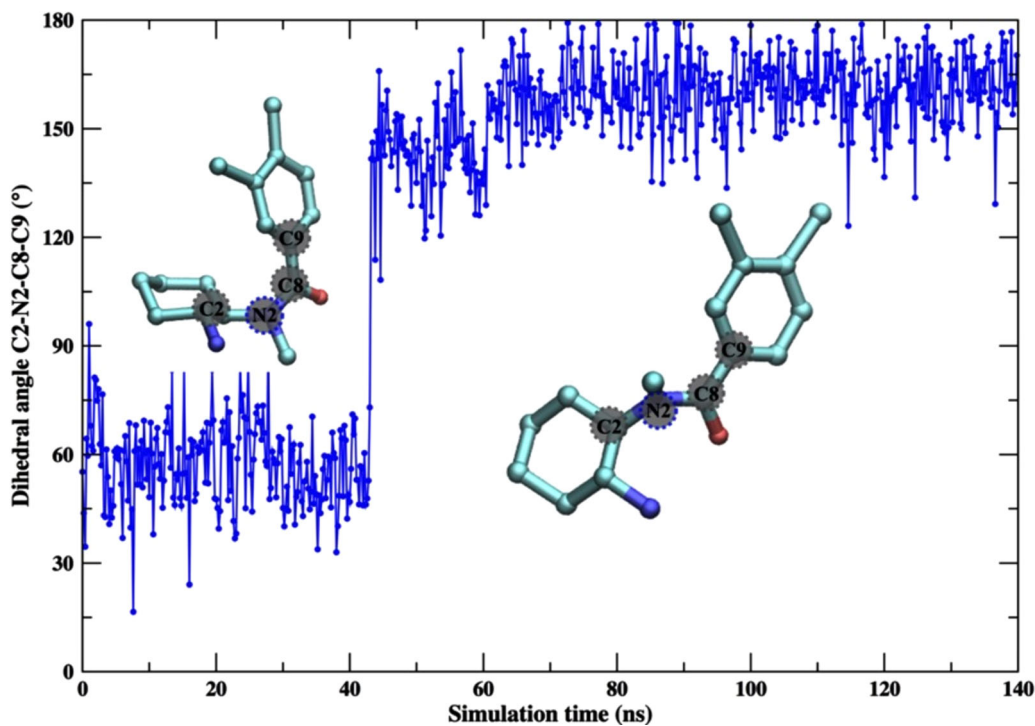


FIGURE 7 Plot of backbone ligand dihedral angle (C2-N2)-(C8-C9) versus simulation time. Average representative ligand structure is also reported before and after simulation time $t = 45$ ns.

TABLE 3 Hydrogen bond network analysis between residues of MOR (first column) and atoms of *N,N*-didesmethyl U-47700 (second column) in two simulation temporal ranges: 0–45 ns (third column) and 45–140 ns (fourth column).

MOR	<i>N,N</i> -didesmethyl U-47700 (LIG)	0–45 ns	45–140 ns
TRP229 (N1)	LIG (O1)	Yes	Absent
TYR262 (OH)	LIG (N1)	Yes	Reduced occupancy
ASP83 (C)	LIG(N1)	Yes	Reduced occupancy
ASP83 (O2)	LIG(N1)	Yes	Yes
ASP83 (O1)	LIG(N1)	Yes	Yes
ASP83 (O1)	LIG(C1)	Yes	Yes

Note: For each amino acid, the specific atom or group contributing to the bond is indicated between brackets.

Abbreviation: MOR, mu-opioid receptor; U-47700, *trans*-3,4-dichloro-*N*-[2-(dimethylamino)cyclohexyl]-*N*-methylbenzamide.

weakening of two other H-bonds (Table 3), when the ligand switched to the extended conformation. These results are consistent with both docking and biological findings and show how small changes in ligand chemical structure can dramatically decrease MOR affinity for *N,N*-didesmethyl U-47700 as compared to U-47700.

Overall, the detailed analysis of the H-bond network and interaction patterns during MD simulations confirmed the docking results for the interactions between receptor regions A, B, C, D (defined in Section 2.1) and the ligands.

In summary, ligand–receptor–membrane interaction energies were able to distinguish between the highest- and lowest-scoring ligands for MOR and KOR. Additionally, when MOR and KOR were each bound to their top-ranking ligand, both receptors displayed a lower propensity to interact with the membrane. Thus, a role for less ligand–receptor–membrane interactions in ligand–receptor binding was revealed. The propensity of the receptor to interact with membrane components is determined by dynamic conformational changes occurring during the molecular recognition and final docking of the ligand. The highest-scoring ligands formed stronger bonds with their respective receptors and thus induced relevant conformational changes. This effect, in turn, led to a less favorable receptor surface for chemical interaction with the membrane.

3 | CONCLUSION

The presented original *in silico* data support the known pharmacological profiles for the opioid receptor ligands U-47700, *N,N*-didesmethyl U-47700, and U-50488.^[10,20] From the docking experiments, it appears that the unique ligand orientation within MOR and KOR is a main factor for receptor affinity determination. For *N,N*-didesmethyl U-47700 binding at MOR, the loss of affinity is likely

related to its strong interaction with the electrostatic region A, while for U-50488 it could be due to its outward shift in the MOR-binding pocket. For U-50488 binding at KOR, the additional methylene group moved the benzene ring outward, providing additional important contacts with the residues of KOR that might engender its higher affinity for the receptor.

The *in silico* experiments suggested a crucial role of the plasma membrane in determining the affinities and selectivity of U-compounds for MOR and KOR. In this regard, we found that ligand–receptor complex formation may reduce the interaction energy with the membrane, even when the interaction energy between ligand and receptor increases. This reflects the tendency towards a global minimum energy state for the entire system and can be simulated by dynamic modeling techniques such as MD that we employed.

Collectively, it seems that the reason for ligand specificity at a particular opioid receptor is inextricably linked to the receptor interaction propensity for the membrane. Top-ranking ligands engage the receptor via stronger binding. Such binding reduces the receptor propensity to interact with the membrane. Based on the MD findings, we were able to identify an extended conformation of *N,N*-didesmethyl U-47700 docked to MOR, not otherwise accessible from the static docking analysis. The extended ligand–receptor conformation for the *N,N*-didesmethyl analog explains reduced MOR affinity, secondary to the loss of one H-bond and the weakening of two others. Interestingly, none of the critical H-bonds are found within the MOR-binding pocket.

Ligand affinities for receptors are mainly explained in terms of H-bond networks. In detail, MOR showed similar hydrogen-bonding interaction networks with both U-47700 and U-50488, whereas the contacts of the Asp147 (region A) backbone atoms differentiated the two ligands, with U-50488 displaying interactions only with Asp147 sidechain atoms. KOR presented a quite distinct H-bond interaction network with the two ligands. Specifically, the interaction with KOR Asn141 (region B) was determinant for U-47700, while the key contact for U-50488 was with Asp138 (region A). Thus, our observations identified receptor region A as the main area affecting affinity. Moreover, the membrane interaction energy analysis confirmed both the sensitivity and the speed of this technique to highlight, within a reasonable simulation time, small but functionally meaningful changes in ligand–receptor binding.

In conclusion, our findings suggest that our *in silico* approach might be a useful tool for the characterization of opioid receptors ligands and for the prediction of novel structures with an improved pharmacological profile.

4 | EXPERIMENTAL

4.1 | Molecular docking methods

The following protocol was used to prepare the simulated systems.^[35–37] The MOR and KOR models were built from the crystallographic

structures of *M. musculus* MOR (PDB ID 6DDF)^[23] and *H. sapiens* KOR (PDB ID 6VI4) coupled to their G-proteins.^[24] The MOR and KOR were crystallized in the active state with the agonist [D-Ala², N-MePhe⁴, Gly-ol]-enkephalin (for MOR) or the agonist (3R)-7-hydroxy-N-((2S)-1-[(3R,4R)-4-(3-hydroxyphenyl)-3,4-dimethylpiperidin-1-yl]-3-methylbutan-2-yl)-1,2,3,4-tetrahydroisoquinoline-3-carboxamide (for KOR) occupying the binding site.^[23,24]

To prepare the receptor docking models, the two PDB structures were treated using the “Protein Preparation Wizard” function^[38–40] within Schrodinger Suite (Schrödinger Release 2018-4: Schrödinger, LLC, New York, NY, 2020). This function sets the protonation states of all titratable residues within the protein structure and performs hydrogen optimization and energy minimization, removing any eventual steric clash. Water molecules present in the crystallographic structures were removed.

Then, ligands were prepared and docked with the Schrodinger Suite-Schrödinger Release 2018-4. In detail, U-47700, *N,N*-didesmethyl U-47700, and U-50488 were prepared with “LigPrep” function that minimize the structure and assign protonation state and bond orders. Ligands have been optimized at physiological pH (pH 7.0 ± 1.0) with the Epik algorithm, generating the het states and then, docked by means of the Glide-XP algorithm^[25] with optimized potentials for liquid simulations (OPLS3e force field.^[26] Restrained energy minimization was applied on hydrogens only using the OPLS3e force field. Prepared protein systems were further checked by Ramachandran plots, ensuring there were no steric clashes. All compounds were placed in the docking box (inner box size 10 × 10 × 10 Å³, outer box 25 × 25 × 25 Å³) with the hydrogen in the axial position and the R-group in the equatorial position. In particular, the following parameters were employed: default scaling of Van der Waals radii (scaling factor of 0.80, partial charge cutoff of 0.15), dock flexibly, edit ligand feature of positional constraints like a donor, perform postdocking minimization, and keep 100% of scoring compounds. All protonated compounds were docked in both protomeric states, and the lowest average docking score was used. The method was validated by docking a series of 11 distinct fentanyl analogs with well-known affinities and selectivity (see Supporting Information).

4.2 | MDs methods

As for docking, we used the MOR 3.5 Å resolution cryoelectron microscopy structure with PDB ID 6DDF^[23] and the KOR 3.3 Å resolution structure with PDB ID 6VI4.^[24] The receptor–ligand complexes were obtained from molecular docking as previously explained. Each receptor–ligand complex was inserted into an equilibrated solvated lipid bilayer consisting of 434 molecules of palmitoyl-oleoyl-phosphatidyl-choline (POPC) and 18,500 water molecules. The overlapping POPC molecules were removed using an in-house script. The relaxed membrane–water system was considered for the subsequent MD simulation of the receptor–ligand complex

embedded in the membrane. As usual, for each system, charges were neutralized by adding counterions. The details of the simulation systems investigated in our study are summarized in Table 1.

The Amber forcefield^[41] was used to simulate the receptor and POPC lipids. For all the ligands analyzed, the charges and the forcefield parameters were obtained following the standard Amber protocol.^[42] An initial energy minimization of the system was performed. This was followed by a constant number of atoms, volume, and temperature run for 0.8 ns at 300 K to relax the protein–membrane interface by applying positional restraints on the protein, water molecules, and lipid head group atoms. Each system was further equilibrated using a constant number, pressure, and temperature run (NPT) at 1 atm pressure and 300 K, with gradual release of the harmonic positional restraints. Further equilibrium of the system was performed using NPT run for 10 ns with all atoms unrestrained, finally followed by 100 ns of the production run. All the simulations were performed using nanoscale molecular dynamics (NAMD) software^[43] and running on a cluster of 60 processors.

The interaction energies for the systems ligand–receptor, membrane–receptor, and membrane–receptor–ligand were calculated by evaluating the nonbonded energy values including Van der Waals and electrostatic energy, using the energy plugin of NAMD software.^[40] A cut-off distance of 10 Å was used for nonbonded interactions. For electrostatic interactions, we adopted the particle mesh Ewald scheme, as described in our previous study.^[44] It is important to mention that the interaction energy scheme adopted in our calculations provides only an estimate in terms of enthalpic contributions to binding, as solvent effects are not explicitly included. Nonetheless, the scheme proved in the literature to be quite effective for ranking the different systems based on their complexation energy values.^[45]

The hydrogen bond interaction network between receptor and ligand was also evaluated, along the simulation time, by using a geometrical criterion, with a donor–acceptor cutoff distance of 3.1 Å and donor–hydrogen–acceptor cut-off angle of 130°.^[44]

ACKNOWLEDGMENTS

Enrico Pieroni and Amit Kumar acknowledge the use of the CRS4 computational facilities and the support by the CRS4 HPC group. Enrico Pieroni acknowledges Sardegna Ricerche and Sardinia Region for partial funding of this research. The research program of Michael H. Baumann is generously supported by NIDA grant DA-000523-14. Graziella Tocco, Maria A. De Luca, and Antonio Laus have been funded by a project from the European Commission under the Call JUST-2017-AGDRUG SUPPORTING INITIATIVES IN THE FIELD OF DRUGS POLICY, JUST-2017-AG-DRUG (Grant agreement no. 806996-JUSTSO). Maria A. De Luca and Antonio Laus also acknowledge the Drug Policies Department, Presidency of the Council of Ministers, Italy (project: “Implementazione dell'identificazione e studio degli effetti delle NPS: Sviluppo di una multicentrica di ricerca per potenziare la base dati dell'Osservatorio Nazionale Tossicodipendenze e del Sistema di Allerta Precoce” (Unit Leader for University of Cagliari, Prof. MA De Luca).

CONFLICTS OF INTEREST STATEMENT

The authors declare no conflicts of interest.

ORCID

Amit Kumar  <http://orcid.org/0000-0002-2547-0071>

Graziella Tocco  <http://orcid.org/0000-0003-0081-5704>

REFERENCES

- [1] M. Waldhoer, S. E. Bartlett, J. L. Whistler, *Annu. Rev. Biochem.* **2004**, *73*, 953. <https://doi.org/10.1146/annurev.biochem.73.011303.073940>
- [2] M. H. Baumann, G. Tocco, D. M. Papsun, A. L. Mohr, M. F. Fogarty, A. J. Krotulski, *Brain Sci.* **2020**, *10*(11), 895. <https://doi.org/10.3390/brainsci10110895>
- [3] K. K. Sharma, T. G. Hales, V. J. Rao, N. NicDaeid, C. McKenzie, *Forensic Toxicol.* **2019**, *37*(1), 1. <https://doi.org/10.1007/s11419-018-0454-5>
- [4] P. Armenian, K. T. Vo, J. Barr-Walker, K. L. Lynch, *Neuropharmacology* **2018**, *134*(Pt A), 121. <https://doi.org/10.1016/j.neuropharm.2017.10.016>
- [5] F. I. Carroll, A. H. Lewin, S. W. Mascarella, H. H. Seltzman, P. A. Reddy, *Ann. N. Y. Acad. Sci.* **2012**, *1248*, 18. <https://doi.org/10.1111/j.1749-6632.2011.06199.x>
- [6] P. F. Von Voigtlander, R. A. Lewis, *Prog. Neuro-Psychopharmacol. Biol. Psychiatry* **1982**, *6*(4-6), 467. [https://doi.org/10.1016/s0278-5846\(82\)80130-9](https://doi.org/10.1016/s0278-5846(82)80130-9)
- [7] P. F. Von Voigtlander, R. A. Lahti, J. H. Ludens, *J. Pharmacol. Exp. Ther.* **1983**, *224*(1), 7.
- [8] M. H. Baumann, S. Majumdar, V. Le Rouzic, A. Hunkele, R. Uprety, X. P. Huang, J. Xu, B. L. Roth, Y.-X. Pan, G. W. Pasternak, *Neuropharmacology* **2018**, *134*(Pt A), 101. <https://doi.org/10.1016/j.neuropharm.2017.08.016>
- [9] E. T. Michalson, J. Szmuszkovicz, in *Progress in Drug Research* (Ed: E. Jucker), Birkhäuser, Basel **1989**, pp. 135–149. https://doi.org/10.1007/978-3-0348-9146-2_6
- [10] M. T. Truver, C. R. Smith, N. Garibay, T. A. Kopajtic, M. J. Swortwood, M. H. Baumann, *Neuropharmacology* **2020**, *177*, 108195. <https://doi.org/10.1016/j.neuropharm.2020.108195>
- [11] J. Szmuszkovicz, *Prog. Drug Res.* **1999**, *52*, 167. https://doi.org/10.1007/978-3-0348-8730-4_4
- [12] V. Vecchietti, A. Giordani, G. Giardina, R. Colle, G. D. Clarke, *J. Med. Chem.* **1991**, *34*(1), 397. <https://doi.org/10.1021/jm00105a061>
- [13] B. V. Cheney, J. Szmuszkovicz, R. A. Lahti, D. A. Zichi, *J. Med. Chem.* **1985**, *28*(12), 1853. <https://doi.org/10.1021/jm00150a017>
- [14] J. B. Zawilska, *Front. Psychiatry* **2017**, *8*, 110. <https://doi.org/10.3389/fpsy.2017.00110>
- [15] Drugs.Com. U-47700 (Pink), **2023**. <https://www.drugs.com/illicit/u-47700.html>
- [16] P. Armenian, A. Olson, A. Anaya, A. Kurtz, R. Ruegner, R. R. Gerona, *Ann. Emerg. Med.* **2017**, *69*(1), 87. <https://doi.org/10.1016/j.annemergmed.2016.06.014>
- [17] World Health Organization. *Expert Committee on Drug Dependence Thirty-ninth report*, **2023**. <https://apps.who.int/iris/bitstream/handle/10665/260546/9789241210188-eng.pdf>
- [18] R. Jorge, *EU Early Warning System Alert: U-47,700 in Europe*; European Monitoring Centre for Drugs and Drug Addiction: Lisbon, Portugal, **2016**.
- [19] A. J. Krotulski, A. L. A. Mohr, D. M. Papsun, B. K. Logan, *Drug Test. Anal.* **2018**, *10*, 127. <https://doi.org/10.1002/dta.2228>
- [20] F. Nordmeier, A. Caninaert, C. P. Stove, P. H. Schmidt, M. R. Meyer, N. Schaefer, *Drug Test. Anal.* **2022**, *14*, 713. <https://doi.org/10.1002/dta.3182>
- [21] O. Dror, D. Schneidman-Duhovny, Y. Inbar, R. Nussinov, H. J. Wolfson, *J. Chem. Inf. Model.* **2009**, *49*, 2333. <https://doi.org/10.1021/ci900263d>
- [22] T. Kaserer, K. Beck, M. Akram, A. Odermatt, D. Schuster, *Molecules* **2015**, *20*, 22799. <https://doi.org/10.3390/molecules201219880>
- [23] A. Koehl, H. Hu, S. Maeda, Y. Zhang, Q. Qu, J. M. Paggi, N. R. Latorraca, D. Hilger, R. Dawson, H. Matile, G. F. X. Schertler, S. Granier, W. I. Weis, R. O. Dror, A. Manglik, G. Skiniotis, B. K. Kobilka, *Nature* **2018**, *558*, 547. <https://doi.org/10.1038/s41586-018-0219-7>
- [24] T. Che, J. English, B. E. Krumm, K. Kim, E. Pardon, R. H. J. Olsen, S. Wang, S. Zhang, J. F. Diberto, N. Sciaky, F. I. Carroll, J. Steyaert, D. Wacker, B. L. Roth, *Nat. Commun.* **2020**, *11*, 1145. <https://doi.org/10.1038/s41467-020-14889-7>
- [25] R. A. Friesner, R. B. Murphy, M. P. Repasky, L. L. Frye, J. R. Greenwood, T. A. Halgren, P. C. Sanschagrin, D. T. Mainz, *J. Med. Chem.* **2006**, *49*(21), 6177. <https://doi.org/10.1021/jm051256o>
- [26] E. Harder, W. Damm, J. Maple, C. Wu, M. Rebol, J. Y. Xiang, L. Wang, D. Lupyan, M. K. Dahlgren, J. L. Knight, J. W. Kaus, D. S. Cerutti, G. Krilov, W. L. Jorgensen, R. Abel, R. A. Friesner, *J. Chem. Theory Comput.* **2016**, *12*(1), 281. <https://doi.org/10.1021/acs.jctc.5b00864>
- [27] A. Kumar, F. Delogu, *Sci. Rep.* **2017**, *7*, 42496. <https://doi.org/10.1038/srep42496>
- [28] A. Kumar, P. Melis, V. Genna, E. Cocco, M. G. Marrosu, E. Pieroni, *Mol. BioSyst.* **2014**, *10*(8), 2043. <https://doi.org/10.1039/c4mb00203b>
- [29] P. Procacci, *Curr. Opin. Struct. Biol.* **2021**, *67*, 127. <https://doi.org/10.1016/j.sbi.2020.08.001>
- [30] M. M. Kozlov, F. Campelo, N. Liska, L. V. Chernomordik, S. J. Marrink, H. T. McMahon, *Curr. Opin. Cell Biol.* **2014**, *29*, 53. <https://doi.org/10.1016/j.ceb.2014.03.006>
- [31] M. Simunovic, C. Prévost, A. Callan-Jones, P. Bassereau, *Philos. Trans. R. Soc., A* **2016**, *374*(2072), 20160034. <https://doi.org/10.1098/rsta.2016.0034>
- [32] E. Kritikou, *Nat. Rev. Mol. Cell Biol.* **2007**, *8*, 342. <https://doi.org/10.1038/nrm2166>
- [33] R. A. Corey, O. N. Vickery, M. S. P. Sansom, P. J. Stansfeld, *J. Chem. Theory Comput.* **2019**, *15*(10), 5727. <https://doi.org/10.1021/acs.jctc.9b00548>
- [34] J. Kapla, I. Rodríguez-Espigares, F. Ballante, J. Selent, J. Carlsson, *PLoS Comput. Biol.* **2021**, *17*(5), e1008936. <https://doi.org/10.1371/journal.pcbi.1008936>
- [35] M. A. De Luca, G. Tocco, R. Mostallino, A. Laus, F. Caria, A. Musa, N. Pintori, M. Ucha, C. Poza, E. Ambrosio, G. Di Chiara, M. P. Castelli, *Neuropharmacology* **2022**, *221*, 109263. <https://doi.org/10.1016/j.neuropharm.2022.109263>
- [36] G. Tocco, A. Laus, M. Vanejevs, A. Ture, R. Mostallino, N. Pintori, M. A. De Luca, M. P. Castelli, G. Di Chiara, *Arch. Pharm.* **2023**, *356*(1), 2200432. <https://doi.org/10.1002/ardp.202200432>
- [37] M. H. Deventer, M. Persson, A. Laus, E. Pottie, A. Caninaert, G. Tocco, H. Gréen, C. P. Stove, *Arch. Toxicol.* **2023**, *97*, 1367. <https://doi.org/10.1007/s00204-023-03465-9>
- [38] A. Manglik, A. C. Kruse, T. S. Kobilka, F. S. Thian, J. M. Mathiesen, R. K. Sunahara, L. Pardo, W. I. Weis, B. K. Kobilka, S. Granier, *Nature* **2012**, *485*, 321. <https://doi.org/10.1038/nature10954>
- [39] G. Madhavi Sastry, M. Adzhigirey, T. Day, R. Annabhimoju, W. Sherman, *J. Comput.-Aided Mol. Des.* **2013**, *27*(3), 221. <https://doi.org/10.1007/s10822-013-9644-8>
- [40] W. Huang, A. Manglik, A. J. Venkatakrishnan, T. Laeremans, E. N. Feinberg, A. L. Sanborn, H. E. Kato, K. E. Livingston, T. S. Thorsen, R. C. Kling, S. Granier, P. Gmeiner, S. M. Husbands, J. R. Traynor, W. I. Weis, J. Steyaert, R. O. Dror, B. K. Kobilka, *Nature* **2015**, *524*(7565), 315. <https://doi.org/10.1038/nature14886>
- [41] W. D. Cornell, P. Cieplak, C. I. Bayly, I. R. Gould, K. M. Merz, D. M. Ferguson, D. C. Spellmeyer, T. Fox, J. W. Caldwell, P. A. Kollman, *J. Am. Chem. Soc.* **1995**, *117*, 5179. <https://doi.org/10.1021/ja00124a002>

- [42] J. Wang, R. M. Wolf, J. W. Caldwell, P. A. Kollman, D. A. Case, *J. Comput. Chem.* **2004**, *25*, 1157. <https://doi.org/10.1002/jcc.20035>
- [43] J. C. Phillips, R. Braun, W. Wang, J. Gumbart, E. Tajkhorshid, E. Villa, C. Chipot, R. D. Skeel, L. Kalé, K. Schulten, *J. Comput. Chem.* **2005**, *26*, 1781. <https://doi.org/10.1002/jcc.20289>
- [44] A. Kumar, L. A. Sechi, P. Caboni, M. G. Marrosu, L. Atzori, E. Pieroni, *New J. Chem.* **2015**, *39*, 1355. <https://doi.org/10.1039/C4NJ01903B>
- [45] L. Mollica, S. Decherchi, S. R. Zia, R. Gaspari, A. Cavalli, W. Rocchia, *Sci. Rep.* **2015**, *5*, 11539. <https://doi.org/10.1038/srep11539>

SUPPORTING INFORMATION

Additional supporting information can be found online in the Supporting Information section at the end of this article.

How to cite this article: A. Laus, A. Kumar, P. Caboni, M. A. De Luca, M. H. Baumann, E. Pieroni, G. Tocco, *Arch. Pharm.* **2023**;356:e2300256.
<https://doi.org/10.1002/ardp.202300256>